Clinical Oral Investigations (2022) 26:2441–2451
https://doi.org/10.1007/s00784-021-04210-1

ORIGINAL ARTICLE

Efficacy of the dual-action GA-KR12 peptide for remineralising initial enamel caries: an in vitro study

John Yun Niu[1,2] · Iris Xiaoxue Yin[1] · William Ka Kei Wu[3] · Quan-Li Li[4] · May Lei Mei[1,5] · Chun Hung Chu[1]

Received: 16 June 2021 / Accepted: 26 September 2021 / Published online: 12 October 2021

Abstract

Objective To investigate the antibiofilm and remineralising effects of the dual-action peptide GA-KR12 on artificial enamel caries.

Materials and methods Enamel blocks with artificial caries were treated with sterilised deionised water as control or GA-KR12. The blocks underwent biochemical cycling with *Streptococcus mutans* for 3 weeks. The architecture, viability, and growth kinetics of the biofilm were determined, respectively, by scanning electron microscopy (SEM), confocal laser scanning microscopy, and quantitative (culture colony-forming units, CFUs). The mineral loss, calcium-to-phosphorus ratio, surface morphology, and crystal characteristics of the enamel surface were determined, respectively, using micro-computed tomography, energy dispersive spectroscopy, SEM, and X-ray diffraction (XRD).

Results SEM showed confluent growth of *S. mutans* in the control group but not in the GA-KR12-treated group. The dead-to-live ratios of the control and GA-KR12-treated groups were 0.42 ± 0.05 and 0.81 ± 0.08, respectively ($p < 0.001$). The log CFUs of the control and GA-KR12-treated groups were 8.15 ± 0.32 and 6.70 ± 0.49, respectively ($p < 0.001$). The mineral losses of the control and GA-KR12-treated groups were 1.39 ± 0.09 gcm^{-3} and 1.19 ± 0.05 gcm^{-3}, respectively ($p < 0.001$). The calcium-to-phosphorus molar ratios of the control and GA-KR12-treated groups were 1.47 ± 0.03 and 1.57 ± 0.02, respectively ($p < 0.001$). A uniformly remineralised prismatic pattern on enamel blocks was observed in the GA-KR12-treated but not in the control group. The hydroxyapatite in the GA-KR12-treated group was better crystallised than that in the control group.

Conclusion The dual-action peptide GA-KR12 inhibited the growth of *S. mutans* biofilm and promoted the remineralisation of enamel caries.

Clinical relevance GA-KR12 potentially is applicable for managing enamel caries.

Keywords Caries · Prevention · Remineralisation · Demineralisation · Peptides · Antimicrobial · Enamel

Introduction

Dental caries is perhaps the most prevalent chronic disease worldwide [1]. Untreated caries can cause pain and spread infection and significantly affect people's general health [2]. During the progress of dental caries, an ecological imbalance occurs between bacterial biofilms and tooth minerals [3]. Acid-producing oral plaque biofilm mainly causes loss of tooth minerals and caries. *Streptococcus mutans* is the most important odontopathogen involved in the initiation and progression of caries [4]. In addition, effective regaining of minerals can reverse the early stage of dental caries [5]. Overall, controlling cariogenic biofilm and promoting tooth remineralisation are essential for managing early caries.

✉ May Lei Mei
may.mei@otago.ac.nz

✉ Chun Hung Chu
chchu@hku.hk

1 Faculty of Dentistry, The University of Hong Kong, Hong Kong, China

2 Department of Oral Medicine, Shanxi Provincial People's Hospital, Taiyuan, Shanxi, China

3 Department of Anaesthesia & Intensive Care, The Chinese University of Hong Kong, Hong Kong, China

4 School of Stomatology, Anhui Medical University, Hefei, Anhui, China

5 Department of Oral Rehabilitation, Faculty of Dentistry, University of Otago, Dunedin, New Zealand

Researchers are developing new strategies to control biofilm and promote mineralisation for caries management.

Researchers are studying different kinds of biomaterials for caries management, such as silver diamine fluoride, bioactive glass, casein phosphopeptide-amorphous calcium phosphate, and antimicrobial peptides [6–9]. Antimicrobial peptides are naturally occurring antimicrobial molecules with broad-spectrum activity. Antimicrobial peptides attack multiple hydrophobic and polyanionic bacterial targets, making it difficult for bacterial mutants resistant to antimicrobial peptides to arise [10]. In addition, the structure of antimicrobial peptides is flexible and can be modified functionally. Researchers are interested in designing and synthesising bifunctional antimicrobial peptides with mineralising properties [11]. Some dual-action antimicrobial peptides have been developed that showed activity in promoting remineralisation or preventing enamel demineralisation [12, 13]. These studies investigated the mineralising properties of antimicrobial peptides based on chemical models.

In our previous work, we developed an antimicrobial peptide GA-KR12 using gallic acid as the mineralising domain [14]. Gallic acid is a naturally occurring compound found in vegetables and fruits. It has proved to be a practical component for inducing and accelerating mineralisation [15]. KR12 is the shortest active peptide derived from human cathelicidin, LL-37 [16]. It is an ideal template peptide because of its small size, low toxicity, and antimicrobial properties against cariogenic species [17]. Our previous work showed that GA-KR12 is biocompatible and inhibits growth of planktonic cariogenic species [14]. In addition, GA-KR12 can promote remineralisation of the initial enamel lesion in a chemical model.

A biochemical cycling model is a combination chemical and biological model that not only provides periodic pH alternation but also supplies a microbiological environment for bacterial impact [18]. Therefore, we investigated the antibiofilm and remineralising effects of GA-KR12 on artificial enamel caries using a biochemical cycling model in the current study. We hypothesised that GA-KR12 could inhibit the growth of *S. mutans* biofilm on the enamel surface and promote remineralisation of artificial enamel caries caused by *S. mutans* biofilm.

Materials and methods

Peptide synthesis

The peptide GA-KR12 was designed by grafting gallic acid to the N-terminal of peptide KR12 (KRIVQRIKDFLR). GA-KR12 was synthesised by standard solid-phase peptide synthesis using standard fluorenylmethoxycarbonyl (Fmoc) chemistry. The purity and molecular weight of peptides were determined through high-performance liquid chromatography (HPLC) and mass spectrometry (MS), respectively [19]. The peptide was dissolved by sterile deionised water for subsequent studies.

Preparing blocks with artificial caries

This study was approved by the Institutional Review Board of the University of Hong Kong/Hospital Authority Hong Kong West Cluster (UW17-511). The study protocol is shown in Fig. 1. Enamel slices (2-mm thick) were prepared from extracted sound human molars. The enamel slices were polished with microfine 4000-grit sandpaper and checked with a stereomicroscope to exclude cracked slices. Twenty-two well-polished enamel slices with no cracks were collected. Each slice was sectioned into two blocks and allocated into one of two groups. All of the blocks were half-covered with acid-resistant nail varnish (Clarins, Paris, France) as the internal control. The blocks were sterilised by autoclaving at 121 °C before use [20].

The bacteria *Streptococcus mutans* American Type Culture Collection (ATCC) 35,668 was used in this study. Each enamel block was soaked in 1 mL *S. mutans* culture (10^8 cells/mL) in brain heart infusion (BHI) broth with 5% sucrose. The enamel blocks were anaerobically incubated at 37 °C for 7 days. The culture medium was refreshed every 2 days. SkyScan 1076 micro-computed tomography (micro-CT) was used to determine the depth of the demineralisation zone (artificial caries) on the exposed surface of the enamel. The blocks were washed ultrasonically and sterilised via autoclaving at 121 °C before biochemical cycling.

Experimental treatment

A 21-day biochemical cycling model at 37 °C was employed to mimic conditions for high caries risk [18]. The cycling procedure included 8-h chemical remineralisation in artificial saliva solution (pH 7.0) followed by 16 h of *S. mutans* biofilm challenge. The formula for the artificial saliva was 20 mM 4-(2-hydroxyethyl)-1-piperazineethanesulfonic acid, 1.5 mM calcium chloride, 0.9 mM potassium dihydrogen phosphate, and 150 mM potassium chloride [21]. The bacteria medium was BHI broth with 5% sucrose, and the concentration of bacterial culture was 10^8 cells/mL. Before refreshing demineralising and remineralising solutions, the blocks were washed ultrasonically using sterile deionised water and treated with GA-KR12 (640 μM) or with sterile deionised water as control. For each treatment, GA-KR12 or sterile deionised water was applied topically for 5 min using a micro-brush (micro applicator-regular; Premium Plus International Ltd., Hong Kong, China). The average amount of GA-KR12 and sterile deionised water was measured by calculating the difference in weight of the

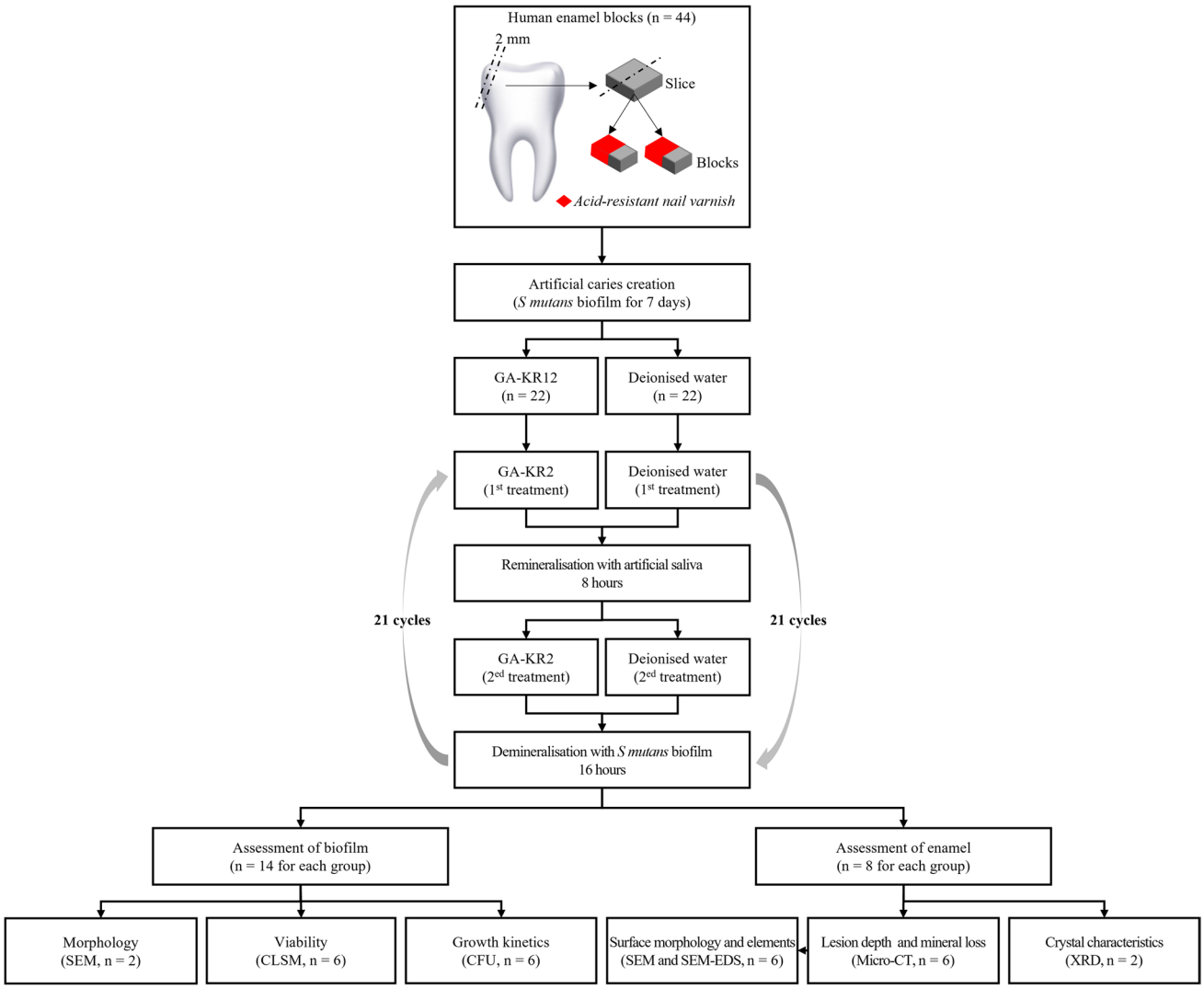

Fig. 1 Flow chart of the study

micro-brush before and after application ten times. After the 21-day biochemical cycling procedure, all of the enamel blocks were collected for subsequent assessments (Fig. 1).

Effect of the peptide on biofilm

Biofilm morphology

SEM (Hitachi S-4800 FEG Scanning Electron Microscope; Hitachi Ltd., Tokyo, Japan) was used to examine the biofilm morphology. A standard sample preparation process was conducted before the assessment. Enamel blocks with biofilm (two blocks per group) were fixed in 2.5% glutaraldehyde for 4 h at 4 °C. Subsequently, the enamel blocks were dehydrated, dried, and sputter-coated for SEM evaluation [22].

Biofilm viability

A confocal laser scanning microscope (CLSM FluoView FV1000, Olympus, Tokyo, Japan) was used to assess the viability of the *S. mutans* biofilm. The biofilm on the enamel surface (six blocks per group) was stained using propidium iodide and SYTO™ 9 dye (LIVE/DEAD BacLight Bacterial Viability Kit, Molecular Probes, Eugene, OR, USA). The red-to-green ratio of the CLSM images was calculated using ImageJ software (National Institutes of Health, USA) to denote the ratio of dead-to-live bacteria [22].

Biofilm growth kinetics

The quantitative culture was used to assess the growth kinetics of the *S. mutans* biofilm. Biofilm from each enamel block (six blocks per group) was collected and resuspended in

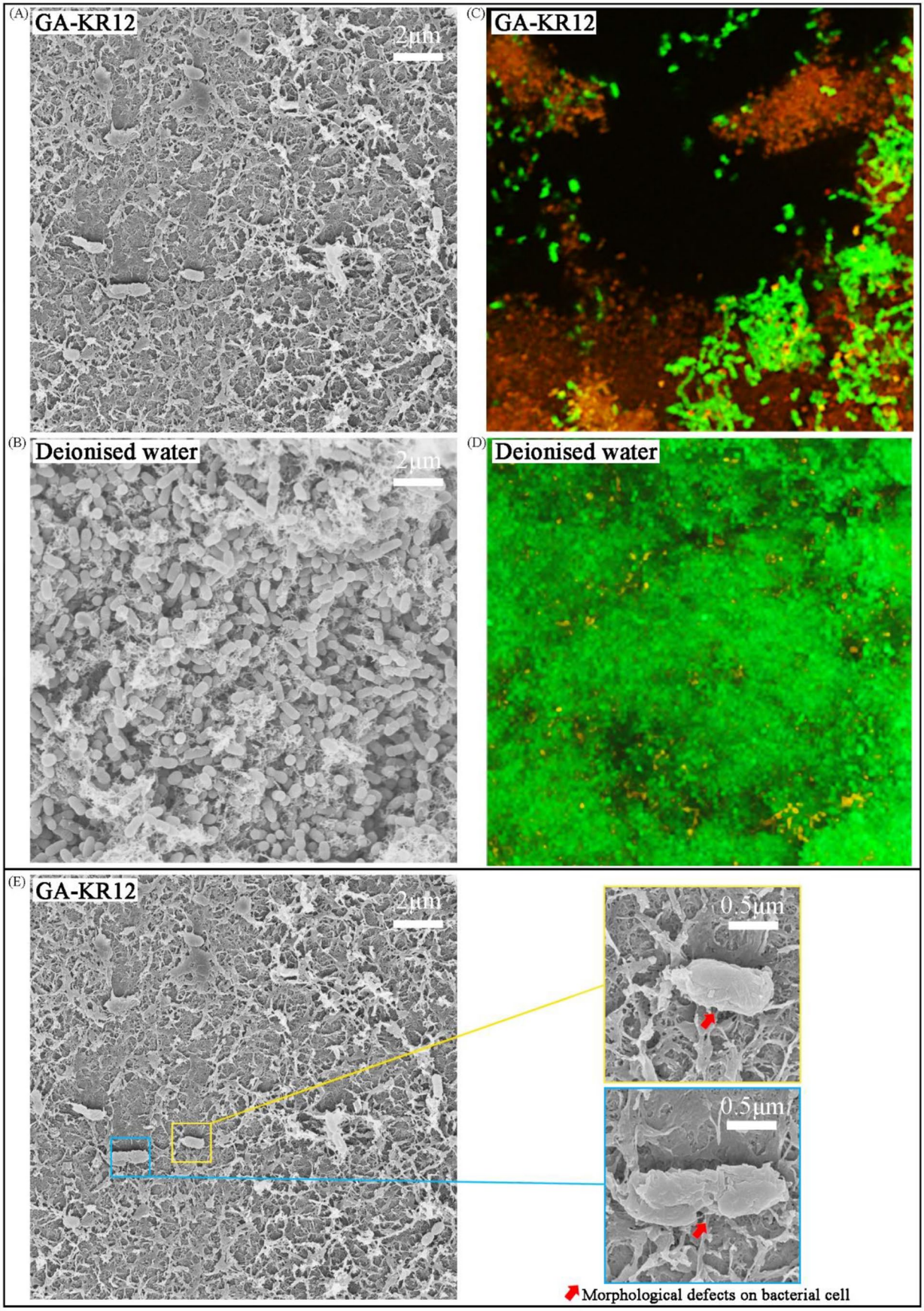
(A)
GA-KR12
2μm
(C)
GA-KR12
(B)
Deionised water
2μm
(D)
Deionised water
(E)
GA-KR12
2μm
0.5μm
0.5μm
Morphological defects on bacterial cell

◂ **Fig. 2** SEM images (×5000) and CLSM images (×100) of *S. mutans* biofilm of the two groups

1 mL BHI broth. The bacteria suspension then underwent ten-fold serial dilution. Ten microliters of each dilution were placed on blood agar and anaerobically incubated at 37 °C for 48 h before colony-forming units (CFUs) were counted. The log CFU was calculated.

Effect of the peptide on hard tissue

Lesion depth and mineral loss

Micro-CT was used to measure the lesion depth and mineral loss of the enamel blocks (six blocks per group). Two standard phantoms (Bruker, Kontich, Belgium) with mineral density values (MDVs, $gHApcm^{-3}$) of 0.25 $gHApcm^{-3}$ and 0.75 $gHApcm^{-3}$ were used to calibrate the greyscale. CTAn software (SkyScan, Antwerp, Belgium) was used to reconstruct and view the three-dimensional images. ImageJ was used to measure the lesion depth. The greyscale values of the demineralised and internal-control areas of enamel blocks were calibrated and calculated into MDVs using CTAn. The mineral loss = MDV of the control region − MDV of the demineralised region [18].

Morphology and element analyses

SEM (Hitachi S-4800 FEG Scanning Electron Microscope; Hitachi Ltd., Tokyo, Japan) was used to examine the enamel surfaces' morphology. Energy-dispersive X-ray spectroscopy under the SEM was used to analyse the element composition of the enamel surfaces. Six blocks of each group were washed ultrasonically before the assessment to remove the biofilm. They were dried in a desiccator and sputter-coated with gold for SEM evaluation. After the micrograph capture and element analyses of calcium and phosphorus, the calcium-to-phosphorus molar ratio—relating to the solubility of calcium phosphate—was calculated [20].

Crystal characteristics

X-ray diffraction (XRD, Rigaku SmartLab 9 kW with CuKa (l = 1.5418 Å; Bruker AXS GmbH, Karlsruhe, Germany) was used to assess the diffraction patterns of the enamel blocks (two blocks per group). The pattern-collection parameters were as follows: the accelerating voltage and the applied current of the X-ray generator were 45 kV and 200 mA, the range of 2θ was 20 to 60°, the step size was 0.02°, and the scan speed was 2.4 s/step. The International Centre for Diffraction Data (ICDD, PDF-2 Release 2004) were used to check the phase purity and to index the chemical phases [23]. The full width at half the maximum of the reflection peak was measured to evaluate the mineral's crystallinity using Origin software [24].

Sample size calculation and statistical analyses

This study was aimed at detecting a difference of at least 20 µm. For a common standard deviation of 10 µm with a power of 0.80 and $\alpha = 0.05$, the sample size was six in each group. The quality data were analysed using SPSS Statistics 20 (IBM Corporation, Somers, NY, USA). The Shapiro–Wilk test was used to test normality, and two-sample *t*-tests were used for assessing differences between the two groups. The cutoff level was set at 5% significance.

Results

After the 7-day *S. mutans* biofilm challenging, approximately 70 µm in the depth of artificial caries on the exposed surface of the enamel was created (Fig. 3A, B). During the 21-day biochemical cycling procedure, the average amount of GA-KR12 and sterile deionised water applied for each treatment were 0.28 ± 0.18 mg and 0.26 ± 0.12 mg, respectively.

Effect of the peptide on biofilm

The SEM images showed that GA-KR12 inhibited the growth of *S. mutans* biofilm on the enamel surfaces (Fig. 2A). The *S. mutans* treated with GA-KR12 lost its normal morphology (Fig. 2E). In contrast, *S. mutans* biofilm fully covered the enamel surface in the control group (Fig. 2B).

A large number of dead cells with red fluorescence were found on the enamel surfaces in the GA-KR12-treated group (Fig. 2C, D). In comparison, high percentages of green fluorescence, representing living cells, were found on the enamel surfaces in the control group. The dead-to-live ratio in the two groups was 0.81 ± 0.08 and 0.42 ± 0.05, respectively (Table 1, $p < 0.001$). This difference revealed that the percentage of dead cells in the GA-KR12-treated group was higher than that of the control group.

The log CFUs values of *S. mutans* for the two groups are also shown in Table 2. The results show that the bacterial count of the GA-KR12-treated group was significantly lower compared to that of the control group.

Effect of the peptide on hard tissue

The lesion depth and the mineral loss of the two groups are shown in Table 2. The enamel blocks in the GA-KR12-treated group exhibited lower lesion depth and mineral loss amounts than those in the control group. Figure 3 shows the

Table 1 Growth kinetics and viability of *S. mutans* in the biofilm of the two groups ($n=6$)

Treatment	Growth kinetics (Dead-to-live ratio)	Viability (Log CFU)
GA-KR12	0.81 ± 0.08	6.70 ± 0.49
Deionised water (control)	0.42 ± 0.05	8.15 ± 0.32
p value	< 0.001	< 0.001

Table 2 Mean lesion depth, mineral loss, and Ca/P molar ratios of the enamel in the two groups ($n=6$)

Treatment	Lesion depth (μm)	Mineral loss (g cm^{-3})	Ca/P molar ratio
GA-KR12	125 ± 5	1.19 ± 0.05	1.57 ± 0.02
Deionised water (control)	171 ± 7	1.39 ± 0.09	1.47 ± 0.03
p value	< 0.001	< 0.001	< 0.001

typical micro-CT images and reconstructed three-dimensional images of the baseline and two groups.

The calcium-to-phosphorus molar ratios of the two groups are displayed in Table 2. The ratio for the GA-KR12-treated group was significantly higher than that of the control group. In addition, typical SEM images of enamel surface morphology are shown in Fig. 4. In the GA-KR12-treated group, the enamel exhibited a relatively smooth surface (Fig. 4A, B). In contrast, the structure of the enamel prisms in the control group was disorganised, with the destruction of the prisms in both interrod and enamel-rod regions (Fig. 4E, F). In the high-magnification images, the enamel in the GA-KR12-treated group exhibited a relatively intact crystal structure on the enamel rod (Fig. 4C, D), which is a sign of remineralisation. In comparison, the crystal structure in both interrod and enamel-rod regions was destroyed in the control group (Fig. 4G, H). Some mesh-form matters were found in the interrod region (Fig. 4H).

The typical XRD spectra of the enamel blocks in the two groups are shown in Fig. 5. The diffraction peaks at 25.9°, 31.8°, 32.2°, and 34.0° correspond to the reflections of (002), (211), (112), and (202) for hydroxyapatite. The reflections of hydroxyapatite in the GA-KR12-treated group were sharper than those of the control group. The full widths at half maximum of the two groups were 0.260° and 0.293°, respectively.

Discussion

This is the first study to investigate the anti-biofilm and remineralising effects of GA-KR12 on artificial enamel caries. The results showed that GA-KR12 inhibited the growth of *S. mutans* biofilm and promoted remineralisation of the artificial enamel caries.

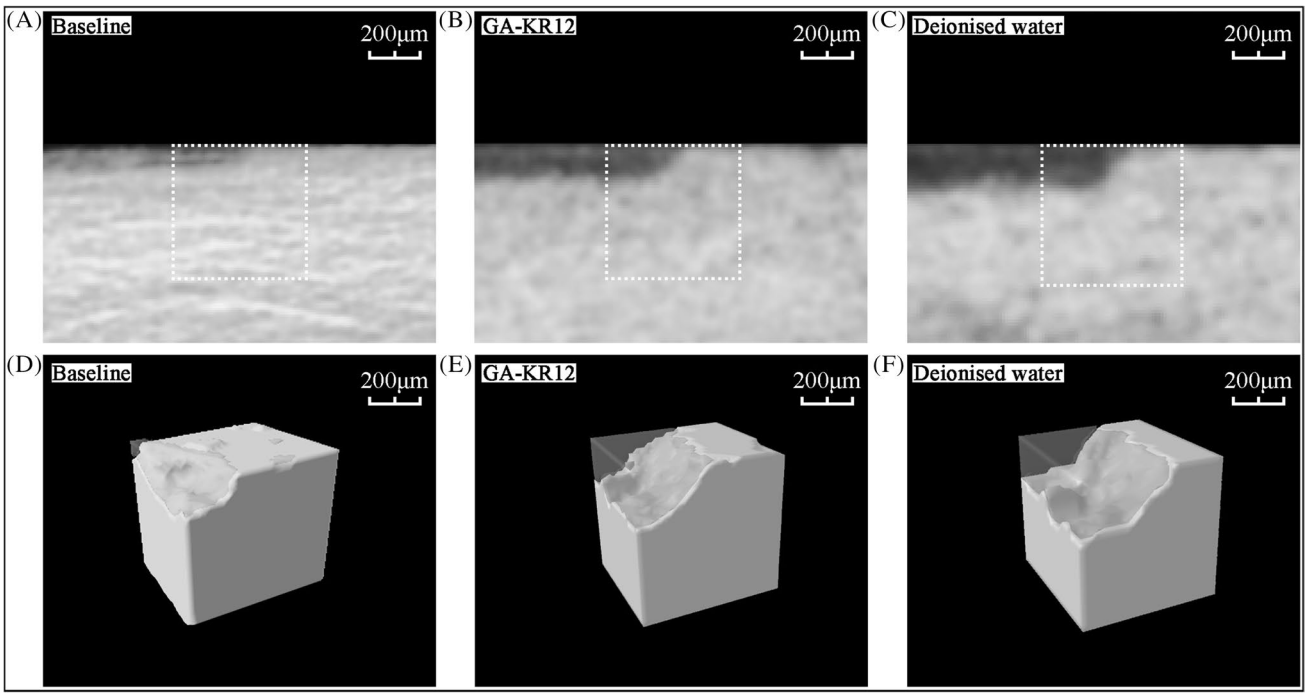

Fig. 3 Micro-CT images (**A**, **B**, and **C**) and reconstructed three-dimensional images (**D**, **E**, and **F**) of the two groups

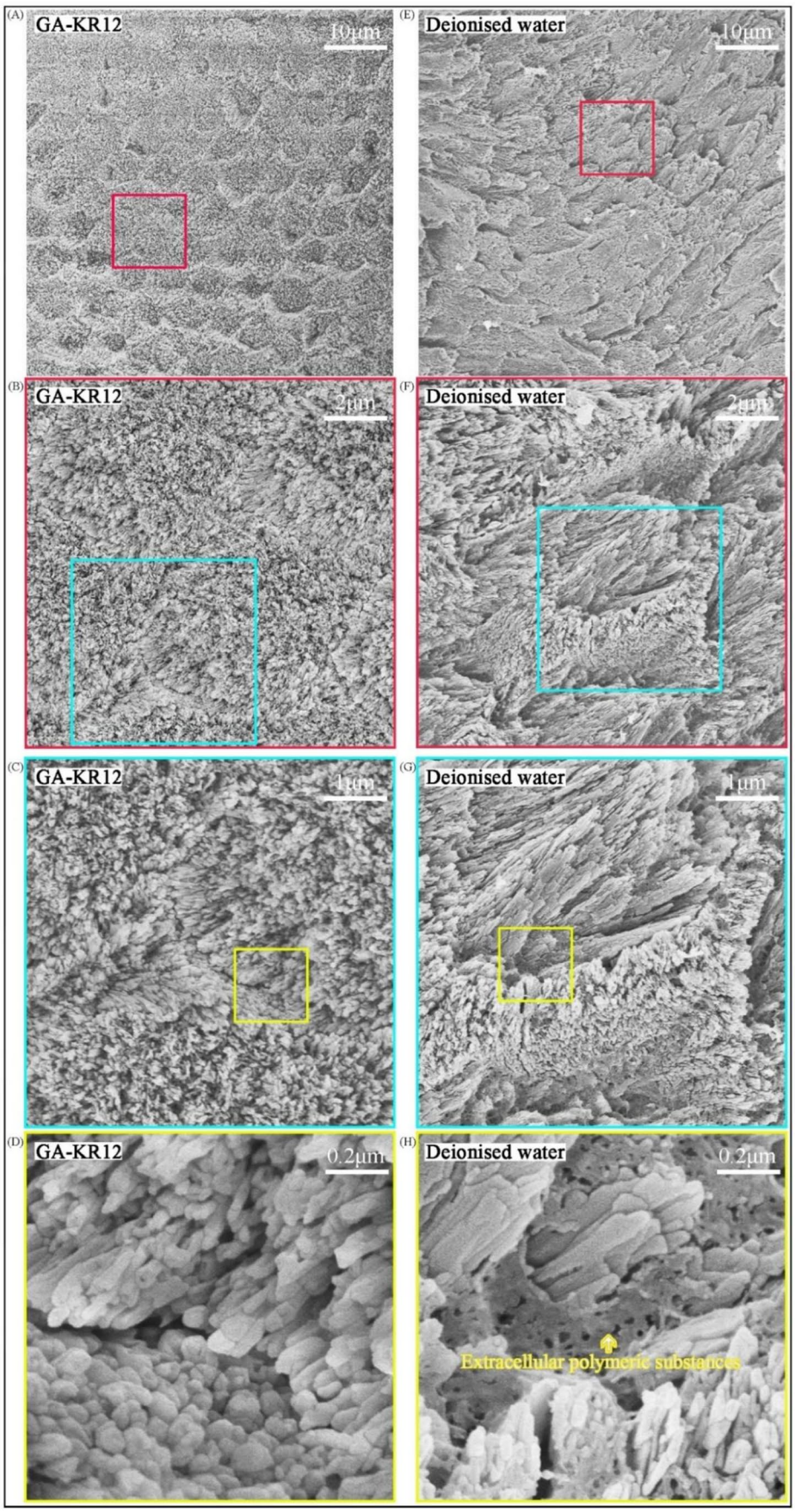

Fig. 4 SEM images (×1000, ×5000, ×10,000, and ×50,000) of enamel surface morphology of the two groups

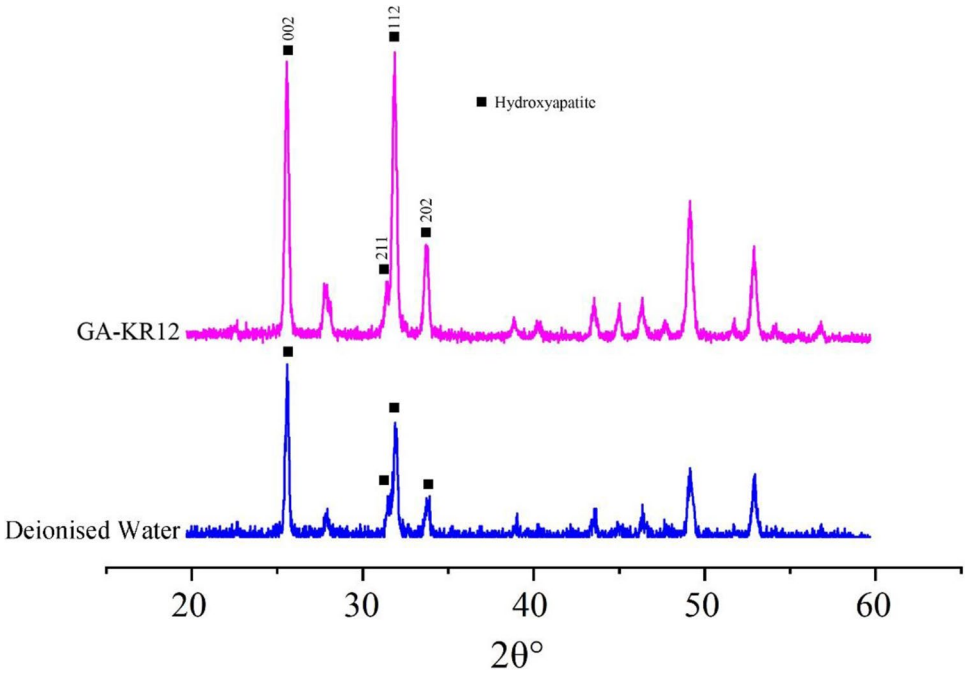

Fig. 5 Typical X-ray diffraction patterns of enamel from a caries lesion

Researchers have tried to develop dual-action antimicrobial peptides to promote remineralisation or prevent enamel demineralisation [12, 13, 25]. One major limitation of these studies is that they investigated the antimicrobial and mineralising properties in separate models, which by no means represent the dual-action effects. Because both effects of a dual-action antimicrobial peptide should be assessed simultaneously, we adopted a biochemical model in this study, which combines biological and chemical factors to mimic an oral environment [18, 26]. A closed *S. mutans* biofilm model system was used to provide a bacterial challenge to demineralisation of the enamel blocks. A 16-h demineralisation process was used to mimic a situation of high caries risk. Artificial saliva was used as the remineralising solution after the demineralising process. Overall, this model provided periodic pH alternation using biological and chemical factors to simulate the initial stage of caries development effectively.

S. mutans is considered the main species causing dental caries. *S. mutans* can colonise the oral cavity and form bacterial biofilm by adhering to the tooth surface. It can produce extracellular polysaccharides to enhance adherence to other plaque bacteria. In addition, *S. mutans* can survive in an acidic environment and produce acid to attack dental hard tissue by fermenting sucrose or other sugars [27]. Thus, *S. mutans* biofilm is the most used microbial model in caries research [28]. We used a biofilm model in a closed system to investigate the bacterial growth and physiological properties of the biofilm because this model is uncomplicatedly repeatable and controllable [28]. However, the interactions among different bacteria cannot be assessed in a monospecies biofilm model.

The peptide GA-KR12 was designed by grafting gallic acid as a mineralising action domain to peptide KR12 as an antimicrobial action domain. Our previous study showed that GA-KR12 inhibited the growth of cariogenic species in planktonic conditions and mineralised initial enamel caries in a chemical model [14]. This study revealed that GA-KR12 significantly inhibited the growth of *S. mutans* biofilm on enamel surfaces. SEM micrographs showed that the GA-KR12 group had less affluent biofilm. In addition, *S. mutans* cells lost their normal shape, and perforations were found on their cell membranes. The antimicrobial peptides might attack hydrophobic and anionic bacterial cell membranes. The cell membranes were then disrupted by the peptides, resulting in leakage of the cytoplasmic content [29]. The CLSM images and log CFU values were consistent, corroborating that the enamel surfaces treated with GA-KR12 had fewer live cells than those treated with deionised water did.

This study revealed that GA-KR12 can inhibit the demineralisation of enamel caries effectively. The mineral content of the enamel blocks was assessed by micro-CT, a nondestructive technique, instead of the traditional polarised light microscope or transverse microradiography [20]. In addition, micro-CT does not require complicated preparation of the enamel blocks. After the micro-CT scanning, a three-dimensional structure can be rebuilt, and quantifiable data such as lesion depth and mineral loss can be calculated. The lesion depth and mineral loss in this study's results indicated that the mineral content of the enamel lesions in the

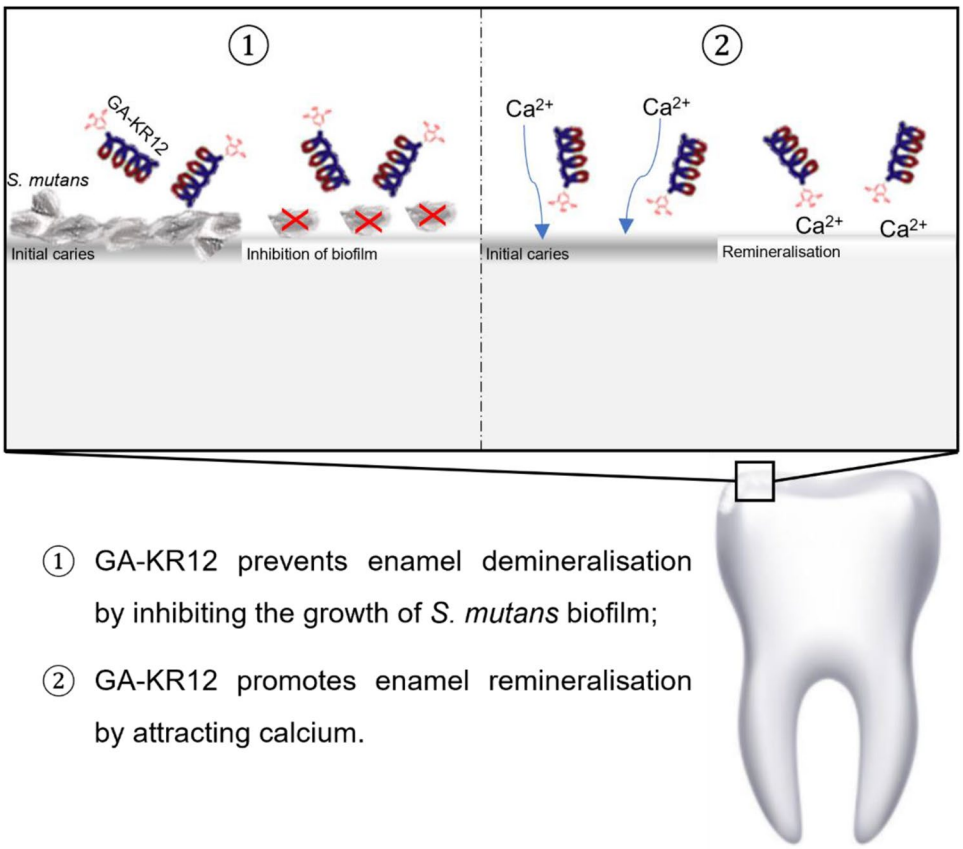

Fig. 6 Dual actions of GA-KR12 for remineralisation of initial enamel caries

GA-KR12 group was significantly greater than those in the deionised water group. In addition, SEM–EDS was used to assess the elemental content on the surfaces of the enamel blocks. SEM–EDS was able to assess the molar and weight percentages of different elements on the enamel surfaces. More phosphate than calcium is lost during demineralisation. An increased calcium-to-phosphorus molar ratio indicates reduced solubility of calcium phosphate compounds [4]. In this study, the calcium-to-phosphorus molar ratio in the GA-KR12 group was significantly higher than that in the deionised water group, consistent with the micro-CT results.

This study showed that the GA-KR12 promoted the remineralisation of enamel caries effectively. We captured low-magnification micrographs (1000×, 5000×) to observe the roughness of the enamel surfaces. The enamel in the GA-KR12 group exhibited relatively smooth surfaces. We observed densely granular structures generated on the enamel surface at high magnification, indicating the remineralisation of the enamel in the GA-KR12 group. In contrast, the blocks in the deionised water group showed rough enamel surfaces, distorted prisms, and damaged crystals. We also found some mesh-formed substances in the interrod region (Fig. 4H), possibly extracellular polymeric substances from biofilm, based on their distinctly meshed structure. A matrix of extracellular polymeric substances is critical in establishing and maintaining the biofilm structure because it facilitates bacterial aggregation and adhesion to form biofilm [30]. The presence of these residual extracellular polymeric substances suggests that the bacteria invaded deep into the enamel due to the dissolution of enamel at the interprismatic region. The XRD spectra of the enamel blocks indicate that the full width at half maximum was lower in the GA-KR12 group than in the deionised water group. A reduced full width at half maximum indicated an increased crystallite size. This is consistent with the SEM results showing that the hydroxyapatite in the GA-KR12 group was better crystallised than that in the deionised water group was.

The dual actions of GA-KR12 for remineralisation of initial enamel caries is shown in Fig. 6. First, GA-KR12 prevented enamel demineralisation by inhibiting the growth of *S. mutans* biofilm. Second, the pyrogallol group of GA-KR12 promoted enamel remineralisation by attracting calcium ions from the remineralising solution. Some remineralising peptides, such as P11-4, also have a high affinity for calcium ions for enamel remineralisation [31]. This dual-action peptide with remineralising and antibacterial properties could be a viable option to remineralise enamel caries.

Conclusion

This study demonstrates that GA-KR12 inhibited the growth of *S. mutans* biofilm and promoted the remineralisation of enamel caries.

Funding This study was supported by a Health and Medical Research Fund (No. 17160402).

Declarations

Conflict of interest The authors declare no competing interests.

References

1. Chen KJ, Gao SS, Duangthip D, Lo ECM, Chu CH (2019) Prevalence of early childhood caries among 5-year-old children: a systematic review. J Investig Clin Dent 10:e12376. https://doi.org/10.1111/jicd.12376
2. Chu CH, Wong SS, Suen RP, Lo EC (2013) Oral health and dental care in Hong Kong. Surgeon 11:153–157. https://doi.org/10.1016/j.surge.2012.12.010
3. Selwitz RH, Ismail AI, Pitts NB (2007) Dental caries. Lancet 369:51–59. https://doi.org/10.1016/S0140-6736(07)60031-2
4. Mei ML, Li QL, Chu CH, Lo EC, Samaranayake LP (2013) Antibacterial effects of silver diamine fluoride on multi-species cariogenic biofilm on caries. Ann Clin Microbiol Antimicrob 12:4. https://doi.org/10.1186/1476-0711-12-4
5. Abou Neel EA, Aljabo A, Strange A, Ibrahim S, Coathup M, Young AM, Bozec L, Mudera V (2016) Demineralization-remineralization dynamics in teeth and bone. Int J Nanomedicine 11:4743–4763. https://doi.org/10.2147/IJN.S107624
6. Mei ML, Lo ECM, Chu CH (2018) Arresting dentine caries with silver diamine fluoride: what's behind it? J Dent Res 97:751–758. https://doi.org/10.1177/0022034518774783
7. Dai LL, Nudelman F, Chu CH, Lo ECM, Mei ML (2021) The effects of strontium-doped bioactive glass and fluoride on hydroxyapatite crystallization. J Dent 105:103581. https://doi.org/10.1016/j.jdent.2021.103581
8. Niu JY, Yin IX, Mei ML, Wu WKK, Li QL, Chu CH (2021) The multifaceted roles of antimicrobial peptides in oral diseases. Mol Oral Microbiol. https://doi.org/10.1111/omi.12333
9. Zhao IS, Mei ML, Burrow MF, Lo EC, Chu CH (2017) Prevention of secondary caries using silver diamine fluoride treatment and casein phosphopeptide-amorphous calcium phosphate modified glass-ionomer cement. J Dent 57:38–44. https://doi.org/10.1016/j.jdent.2016.12.001
10. Andersson DI, Hughes D, Kubicek-Sutherland JZ (2016) Mechanisms and consequences of bacterial resistance to antimicrobial peptides. Drug Resist Updat 26:43–57. https://doi.org/10.1016/j.drup.2016.04.002
11. Niu JY, Yin IX, Wu WKK, Li QL, Mei ML, Chu CH (2021) Antimicrobial peptides for the prevention and treatment of dental caries: a concise review. Arch Oral Biol 122:105022. https://doi.org/10.1016/j.archoralbio.2020.105022
12. Wang X, Wang Y, Wang K, Ren Q, Li H, Zheng S, Niu Y, Zhou X, Li W, Zhang L (2019) Bifunctional anticaries peptides with antibacterial and remineralizing effects. Oral Dis 25:488–496. https://doi.org/10.1111/odi.12990
13. Basiri T, Johnson ND, Moffa EB, Mulyar Y, Serra Nunes PL, Machado M, Siqueira WL (2017) Duplicated or hybridized peptide functional domains promote oral homeostasis. J Dent Res 96:1162–1167. https://doi.org/10.1177/0022034517708552
14. Niu JY, Yin IX, Wu WKK, Li QL, Mei ML, Chu CH (2021) A novel dual-action antimicrobial peptide for caries management. J Dent 111:103729. https://doi.org/10.1016/j.jdent.2021.103729
15. Prajatelistia E, Ju SW, Sanandiya ND, Jun SH, Ahn JS, Hwang DS (2016) Tunicate-inspired gallic acid/metal ion complex for instant and efficient treatment of dentin hypersensitivity. Adv Healthc Mater 5:919–927. https://doi.org/10.1002/adhm.201500878
16. Wang G (2008) Structures of human host defense cathelicidin LL-37 and its smallest antimicrobial peptide KR-12 in lipid micelles. J Biol Chem 283:32637–32643. https://doi.org/10.1074/jbc.M805533200
17. Caiaffa KS, Massunari L, Danelon M, Abuna GF, Bedran TBL, Santos-Filho NA, Spolidorio DMP, Vizoto NL, Cilli EM, Duque C (2017) KR-12-a5 is a non-cytotoxic agent with potent antimicrobial effects against oral pathogens. Biofouling 33:807–818. https://doi.org/10.1080/08927014.2017.1370087
18. Yin IX, Yu OY, Zhao IS, Mei ML, Li QL, Tang J, Lo ECM, Chu CH (2020) Inhibition of dentine caries using fluoride solution with silver nanoparticles: an in vitro study. J Dent 103:103512. https://doi.org/10.1016/j.jdent.2020.103512
19. Cao Y, Liu W, Ning T, Mei ML, Li QL, Lo EC, Chu CH (2014) A novel oligopeptide simulating dentine matrix protein 1 for biomimetic mineralization of dentine. Clin Oral Investig 18:873–881. https://doi.org/10.1007/s00784-013-1035-y
20. Zhao IS, Xue VW, Yin IX, Niu JY, Lo ECM and Chu CH (2021) Use of a novel 9.3-mum carbon dioxide laser and silver diamine fluoride: prevention of enamel demineralisation and inhibition of cariogenic bacteria. Dent Mater. https://doi.org/10.1016/j.dental.2021.02.017
21. Yu OY, Mei ML, Zhao IS, Lo EC, Chu CH (2017) Effects of fluoride on two chemical models of enamel demineralization. Materials (Basel) 10. https://doi.org/10.3390/ma10111245
22. Yin IX, Yu OY, Zhao IS, Mei ML, Li QL, Tang J, Chu CH (2019) Developing biocompatible silver nanoparticles using epigallocatechin gallate for dental use. Arch Oral Biol 102:106–112. https://doi.org/10.1016/j.archoralbio.2019.03.022
23. Yu OY, Mei ML, Zhao IS, Li QL, Lo EC, Chu CH (2018) Remineralisation of enamel with silver diamine fluoride and sodium fluoride. Dent Mater 34:e344–e352. https://doi.org/10.1016/j.dental.2018.10.007
24. Li QL, Ning TY, Cao Y, Zhang WB, Mei ML, Chu CH (2014) A novel self-assembled oligopeptide amphiphile for biomimetic mineralization of enamel. BMC Biotechnol 14:32. https://doi.org/10.1186/1472-6750-14-32
25. Niu JYYI, Wu WKK, Li QL, Mei ML, Chu CH (2021) Data from: a concise review on antimicrobial peptides for prevention and treatment of dental caries. Dryad Dataset. https://doi.org/10.5061/dryad.bvq83bk88
26. Niu JY, Yin IX, Wu WKK, Li QL, Mei ML, Chu CH (2021) Remineralising dentine caries using an artificial antimicrobial peptide: an in vitro study. J Dent 111:103736. https://doi.org/10.1016/j.jdent.2021.103736
27. Krzysciak W, Jurczak A, Koscielniak D, Bystrowska B, Skalniak A (2014) The virulence of Streptococcus mutans and the ability

to form biofilms. Eur J Clin Microbiol Infect Dis 33:499–515. https://doi.org/10.1007/s10096-013-1993-7
28. Yu OY, Zhao IS, Mei ML, Lo EC, Chu CH (2017) Dental biofilm and laboratory microbial culture models for cariology research. Dent J (Basel) 5. https://doi.org/10.3390/dj5020021
29. van't Hof W, Veerman EC, Helmerhorst EJ, Amerongen AV (2001) Antimicrobial peptides: properties and applicability. Biol Chem 382:597–619. https://doi.org/10.1515/BC.2001.072
30. Yin J, Mei ML, Li Q, Xia R, Zhang Z, Chu CH (2016) Self-cleaning and antibiofouling enamel surface by slippery liquid-infused technique. Sci Rep 6:25924. https://doi.org/10.1038/srep25924
31. Wierichs RJ, Carvalho TS, Wolf TG (2021) Efficacy of a self-assembling peptide to remineralize initial caries lesions - a systematic review and meta-analysis. J Dent 109:103652. https://doi.org/10.1016/j.jdent.2021.103652